IEEE Access
Multidisciplinary | Rapid Review | Open Access Journal

Received April 8, 2021, accepted April 23, 2021, date of publication April 27, 2021, date of current version May 5, 2021.

Digital Object Identifier 10.1109/ACCESS.2021.3075960

Development of a High Peak Voltage Picoseconds Avalanche Transistor Based Marx Bank Circuit

RENJIE HE, YANG LI, ZHENNAN LIU, JIAHAO JIN, AND ZHENGCHUN SUN
School of Physics, University of Electronic Science and Technology of China, Chengdu 611731, China
Corresponding author: Yang Li (yli@uestc.edu.cn)

ABSTRACT Avalanche transistor-based Marx bank circuit (MBC) is widely used to generate high voltage nanosecond pulses with high amplitude, high repetition rate, fast rise time, and low jitter. Researchers have tried to modify the circuit structure by using parallel or series avalanche transistors to increase peak power. However, in this work, the detailed process of analyzing and designing a compact Marx generator using avalanche transistors will be described. The purpose of this article is to report our experimental observations on the mechanism of operation of the MBCs. By studying the influence of amplitude and pulse width of the trigger circuit, a Gaussian pulse with a rising edge of 160 ps, full width at half maximum (FWHM) of 660 ps, and amplitude of 5000 V are obtained. The design improves the output voltage and pulse repetition frequency (PRF) effectively while reducing the use of the number of transistors. Based on the conventional principles of avalanche transistors and Marx circuit, a list of useful and interesting conclusions obtained from experiments will be reported.

INDEX TERMS High power pulse source, Gaussian signal, Marx circuit, avalanche transistor.

I. INTRODUCTION

In recent years, avalanche transistors are being widely used to provide both fast response and large peak power because of their fast speed, high stability, and easy cascading [1]. Pulsed power sources made based on avalanche transistors have been widely used in ultra-wideband radar [2], laser pulse switching [3], high-speed camera driving [4], and cellular medicine [1]. The ultra-wideband radar made from them is also used for oil logging and mineral exploration due to the excellent penetration and high-resolution performance [5]. Avalanche transistors can also be used to make pulse sources which can collect pollutants as a gas treatment device to reduce atmospheric pollution as well as being applied to industrial radiography to control smog [6]. One can use a high power pulse source made by avalanche transistors in energy spectrum measurement experiments to provide a nanosecond uniform pulsed electron beam [7]. Many articles on Marx's pulse sourced have been published in recent years. Such as:

Li *et al.* [8] have reported a pulse source with an adjustable range of 1,600 V to 3,000 V considering the design issues, such as the relationship between the pulse parameters and the electroporation effects for applications in the nuclear or cell membrane.

The associate editor coordinating the review of this manuscript and approving it for publication was Pu-Kun Liu.

Yuan *et al.* [9] used a hybrid pulse technique combining the topology utilizing the combination of modularized avalanche transistor Marx circuits, direct pulse adding, and transmission line transformer. The authors reported an output having 2-14 kV amplitude, 7-11 ns width, and a maximum 10 kHz repetitive rate on a matched 50-300 Ω resistive load.

Zhang *et al.* [10] reported the use of the avalanche transistor as the switch of Marx circuit with four high-stability pulse generators combined, which generated a higher peak voltage up to 3.9 kV.

With the development of power electronics, avalanche transistors are becoming more and more suitable for pulsed power applications. They could provide the pulsed power systems with compactness, reliability, high repetition rate, and a long lifetime [8]–[10]. For producing high voltage pulses Marx generator is the most popular and is the most widely used method [11]. It can only get a high amplitude output from a few components, but the circuit's pulse width control is a problem. Numerous publications deal with ways to increase pulse voltage or current amplitudes by connecting multiple avalanche transistors in series, parallel, or configurations such as the Marx bank. Ultra-short pulse generator based on Marx circuit, whose switch is avalanche transistor, could generate a very short pulse with high peak voltage [12], [13]. The ultra-fast rising-edge of the pulse is mainly determined by the transistor's avalanche effect. The circuit's structure has

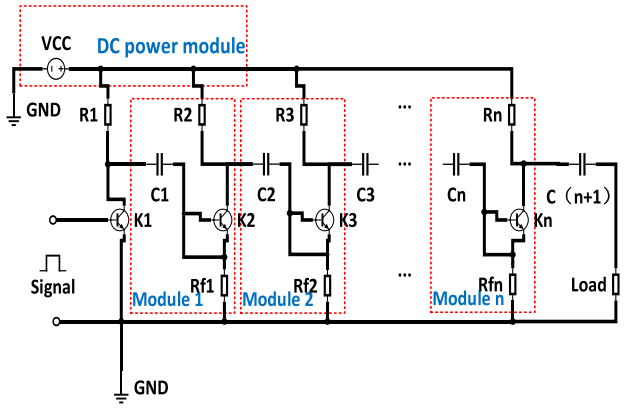

FIGURE 1. Marx circuit schematic diagram.

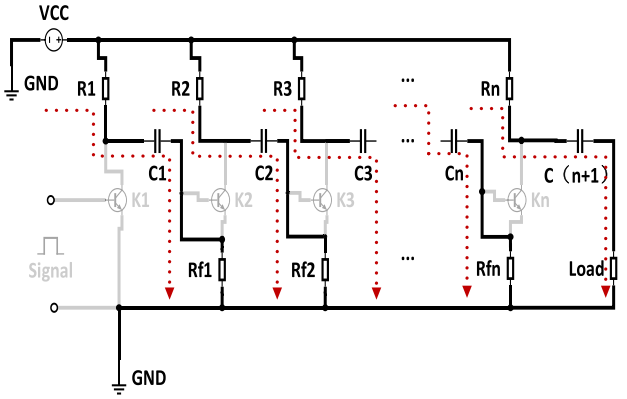

FIGURE 2. The charging phase of the Marx circuit.

been changed from the gap discharge structure to the stable avalanche transistor Marx circuit structure [14]–[17], and the pulse width control has been possible from microsecond, nanosecond to sub nanosecond. After solving the pulse width problem, the next question is how to reduce the pulse width while increasing the pulse source's output. It is difficult to meet all the parameters simultaneously due to the limitations of switching devices [18], [19]. Among various methods to generate nanosecond pulses, the avalanche transistor-based Marx bank circuit (MBC) gives a promising choice, due to the high switching speed of the avalanche transistor and the simplicity of the circuit [20].

Avalanche transistors generally work in high-speed mode and the avalanche transistors' characteristics are different from the ordinary transistors in that the avalanche transistor mainly works in the avalanche region of the transistor. Bipolar transistors operated in avalanche breakdown mode are commonly used to construct pulse generators [21]. By increasing the electric field in the collector junction's space charge region, the electrons collide with the lattice to form a new pair of electron holes. The original pair of electron holes in the space and the new pair move in the opposite direction together. When the reverse voltage increases to a specific value, the carrier doubling situation occurs like an avalanche. It causes the reverse current to rise sharply—thus causing the collector junction breakdown. Thus, one can use the avalanche multiplier effect of transistors to generate a narrow nanosecond pulse with high amplitude. One limiting factor in avalanche transistor circuits based on the basic triggered-switched capacitance-discharge topology is the rate at which the energy storage element at the collector can be recharged [16].

Several reports have been published over these years on the design and performance of different variants of this circuit, but a few analyses of the trigger signals. In this work, the detailed process of analyzing and designing a compact Marx generator using avalanche transistors has been taken up. In this paper, we propose a modification of the circuit structure and trigger circuit architecture to improve the output. Compared with the widely used conventional circuits, the use of a lower number of avalanche transistors reduces the cost and produces a large peak pulse. In the second part, we introduce the circuit stage number selection procedure using the saturation trend curve of Marx structure stages and present the preliminary experimental results from a 40-stage module circuit. In the third part, we introduce the features of the circuit improvements by comparing results from the parallel experiments of capacitors with the conventional single capacitor. In the fourth part, we study the influence of trigger signal on output and present the results from the study using the trigger circuit structure when loaded with an experimental circuit to verify the trigger device's rationality and practicability. Finally, the experimental results are summarized and compared with the existing structures and the conclusions, as well as the complete design process, are discussed.

II. THE CIRCUIT STAGE NUMBERS STUDY

The Marx circuit structure collects charge by capacitors, and the avalanche transistors in the circuit turn on stage by the stage when the trigger signal arrives, releasing large pulses of current at the load. Theoretically, as the stage numbers increases, the pulse amplitude will also increase, but this increase is limiting by the amplitude and will not increase indefinitely [9], [22]. Therefore, it is essential to select the appropriate stages output pulse to obtain the maximum peak power output with saving the devices. After describing the working principle of the Marx circuit, we will deduce the appropriate circuit stage numbers through experiments as the basis of subsequent experiments.

A. THE CHARGING PHASE

When there is no trigger signal input in the circuit, the charging power supply voltage is lower than the bias voltage between the base and collector of the avalanche transistor. At this time, all avalanche transistors Ki on the circuit is in the off state. The current limiting resistors Ri, Rfi, and the energy storage capacitor Ci form the charging path.

B. THE DISCHARGING PHASE

When the trigger voltage signal arrives, the bias voltage between the first avalanche transistor's base and collector

exceeds its avalanche voltage. The first avalanche transistor enters the avalanche state and then conducts rapidly. The trigger signal is passed and drives the subsequent avalanche transistors to work in turn. After the last avalanche transistor is turning on, all energy storage capacitors, avalanche transistors, and load resistors on the circuit form the RC circuit to discharge. And instantly release a pulse signal.

C. THE EXPERIMENT

The conventional approach to increase the output voltage is to use a string of avalanche transistors, or a Marx bank-type design. The Marx bank-type design has the advantage of a lower power supply voltage but at the cost of much more stored charge. According to earlier researchers' observations, we know that the Marx circuit will eventually stabilize the voltage growth with the stage numbers. Thus one needs to find this stability trend. After determining the material's permittivity on the board, we need to select the Marx circuit's grade. The next thing we need to do is find the most appropriate stage number. We set up three controlled experiments to determine the optimal Marx stages setting for the circuit board used. By making a 50-stage board, increasing the Marx circuit stages step by step, and testing, the 50-stage test results are aggregated into a growth curve.

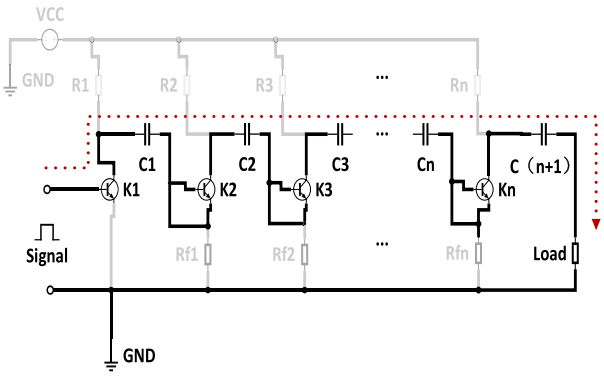

FIGURE 3. The discharge phase process of the Marx circuit.

We used 47 pF, 470 pF, and 1 nF as the control experiment. Setting the resistance value of the Rfi in Fig.3 as 10 kΩ and according to our estimation in (Eqn. 2), the final study's capacitance value should be between these capacitor values. The circuit board's voltage growth characteristics with the same material and wiring form should be consistent with this experiment's trend. The test results are drawn step by step as shown in Fig. 4.

In Fig. 4, we can see that all the three curves in the figure indicate that the output amplitude increases with the increase of the stage number. Still, with the rise of the circuit stage, the output amplitude increases slowly and finally tends to be the same. Among the three curves, from the output curve with a 47pF capacitor, one can observe the output characteristic when the stage numbers are small. The output has a trend to get saturated; this is because the 47 pF capacitor is small, discharge speed is too fast, which increased the resistance

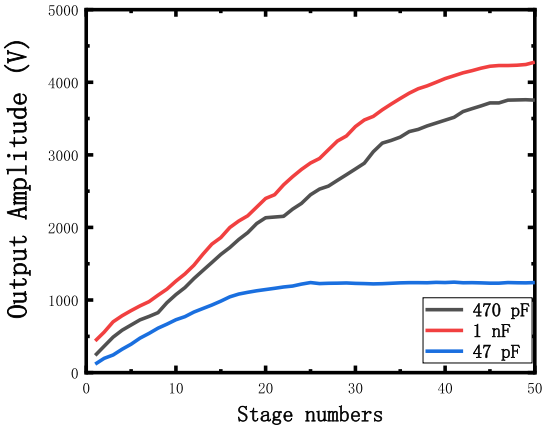

FIGURE 4. Different capacitance values grow with the stages test output results.

of the output circuit leading to stabilization. As the output curve levels off in the end, a continuous increase in series is challenging to increase the total output circuit. In the output curves of 470pF and 1nF capacitors, we can observe that the output curve tends to saturate at the end of the stages.

Due to the small number of stages in the above experiments, the difference in output curve characteristics of 470pF and 1nF is not significant. For the investigation, the circuit board's subsequent output is substantial, and its output trend determines the matching degree of the experimental results in the function fitting. Because there are few reference points at the stable circuit output, the fitting algorithm mainly refers to the points at unstable state output as the basis of function fitting, which will lead to a big difference between the function fitting result and the real situation's production. This will affect the judgment of the overall conclusion. Therefore, the output curve of the 47pF capacitor with the most appropriate fitting effect as a reference for subsequent experiments is considered. Its fitting curve is as follows:

The fitting equation is:

$$y = A \cdot (1 - \exp(-k \cdot (x - xc))) \tag{1}$$

The terms in this equation are

$$A = 1281.67 \quad k = 0.101 \; xc = 0.843$$

And k is the circuit stages number.

As in (Eqn. 1). This shows that there is an upper limit to the total output amplitude as the Marx circuit stages increase.

D. STAGES SELECTION CONCLUSION

According to (Eqn. 1) and the experimental curve, we found that with the increased number of stages, the output signal's peak voltage tends to get saturated. By selecting the number of stages before saturation, the output can be made high enough, and the use of the number of avalanche transistors can be made minimum.

Referring to Fig.4, we found that with the increase of stages, the output signal's peak voltage leads to saturation.

In this experiment, to improve the pulse source output signal's peak voltage as high as possible, we finally selected the Marx circuit of 40 stages to generate the pulse signal.

III. SETTING OF ENERGY STORAGE CAPACITOR

A. CALCULATION OF CAPACITANCE VALUE

Marx circuit technology is now matured since its creation and will not be discussed for the specific index demonstration. The empirical formula of an essential index of the pulse source circuit is shown below to deduce device parameters. Assume that the impulse signal generating circuit consists of N-stage avalanche transistors. When N-stage energy storage capacitors discharge in stages, the energy stored by all energy storage capacitors is equal to κ_ε times of the pulse signal source's output energy [23].

$$C_i = \frac{\sqrt{\pi}}{\sqrt{2ln(1.2)}} \frac{T_e \kappa_\varepsilon U_e^2}{R_l (nU_0)^2} \tag{2}$$

As in (Eqn. 2). Take $\kappa_\varepsilon = 1.2$, $T_e = 0.6$ ns, $U_e = 5$ kV, $U_0 = 300$ V, $R_l = 50\ \Omega$, $n = 40$, and the energy storage capacitor is the same in all the stages, then calculated energy storage capacitor will have a capacitance of $C_i = 284$ pF.

B. CAPACITANCE TYPE STUDY

According to the circuit structure shown in Fig.3, in the last stage of conduction, the whole circuit starts to discharge. Theoretically, the loss of the circuit during discharge comes from the intrinsic impedance of the transistor in the circuit and the equivalent stage resistances, so we infer that the actual voltage obtained at the load end may be calculated using Eqn. 3.

$$U_R = \frac{U_0 \cdot R}{R + nr_d + nr_c} \tag{3}$$

In the formula, U_R is the actual voltage received on the load, R is the load Resistance value, U_0 is the output voltage that Marx circuit can produce, n is the Stages, r_d is the intrinsic impedance of the transistor, and r_c is the equivalent stages resistance, namely ESR(Equivalent Stages Resistance). According to (Eqn. 3), when the stages n is determined, the transistor's selection has been determined and cannot change its inherent resistance r_d This improves the voltage U_R loaded on the load and reduce its loss in each link, however, the experiment can only lower the ESR value, r_c of the capacitor.

In (Eqn. 3), which describes the capacitor's ESR effect on the output, we can make a reasonable choice based on our research to reduce the impact. According to our experimental principle, the impulse signal source's impulse signal can be expressed analytically by the first-order Gaussian function. U_0 is used to represent the maximum value of the first-order Gaussian signal, and T_0 is the half-peak width of the Gaussian pulse.

$$U_0(t) = U_0 exp(-\alpha_0 t^2) \alpha_0 = \frac{4ln2}{T_0^2} \tag{4}$$

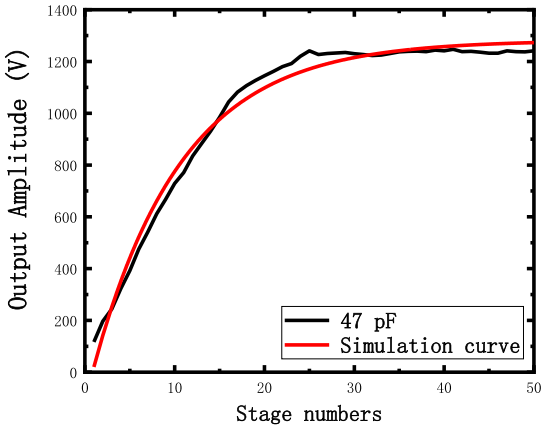

FIGURE 5. Circuit output and fitting curve of 47 pF.

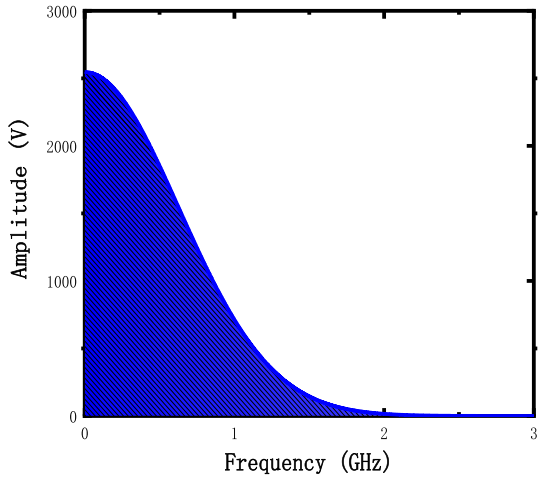

FIGURE 6. The spectrum after the Fourier transform.

After Fourier transform

$$F_0(\omega) = U_0 exp\left(\frac{-\omega^2}{4\alpha_0}\right) \tag{5}$$

Substituting the value $U_0 = 4000$, $T_0 = 0.5$ ns, and we show the spectrum of (Eqn. 5) in Fig.6.

Observing the spectrum distribution in Fig. 6, we can find that the frequency component of the output pulse mainly concentrated in the low-frequency range from 0-1 GHz, so the capacitance with low-frequency loss and for the corresponding frequency band should be selected to meet the experimental requirements to achieve the purpose of improving the circuit performance.

Therefore, the C0G material capacitor with the smallest ESR is selected according to the query of the existing patch capacitor on the market. Then, according to the frequency range in Fig.6 above, the capacitor working at 10 MHz-1000 MHz was selected in detail, and the ESR curves were sorted out as follows.

According to Fig.7, we selected the capacitance value for working in the appropriate frequency band to reduce the influence of ESR of the capacitor in the experiment to make

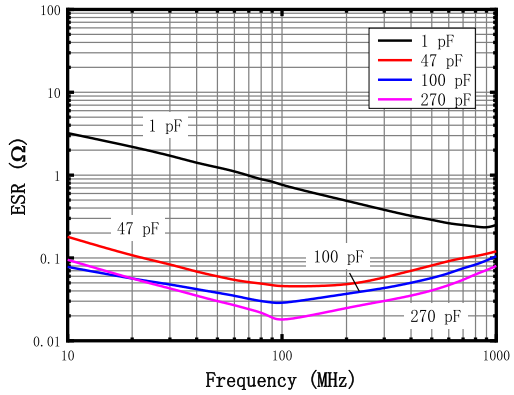

FIGURE 7. ESR curves of different capacitance values.

the load end receive more output. However, the 47 pF capacitance curve and the 270 pF capacitance curve are too close to distinguish improvement in practical applications. Then we set the experiment of six stages of parallel capacitance. The experiment was performed to increase the capacitance, reduce its own ESR, discuss the situation that it is not in parallel, and find out the most appropriate scheme to improve the output, which is the purpose of the design of this experiment.

C. EXPERIMENT AND CONCLUSION

After setting the shunt capacitor structure, the same Marx circuit board was used for the comparative experiment. Since a 282 pF capacitor was not available in the market, we selected a similar situation for a relative verification. A shunt capacitor group of 6* 47 pF and a single energy storage capacitor of 300 pF and 270 pF were chosen for the comparative experiment. To intuitively reflect the data difference, the oscilloscope waveform is shown in Fig.8.

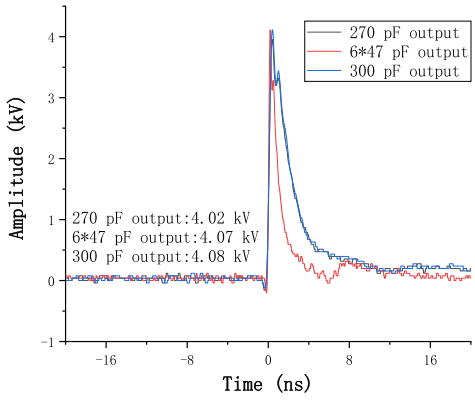

FIGURE 8. Output curves of different capacitance values.

In control experiments, all other components being equal, we can see from the contrast curves in Fig. 8, multiple parallel capacitor output amplitude curves are better than a single capacitor output amplitude curve. It is also observed that the output of the 300 pF capacitor and the output of the parallel capacitance are the same, but we observe a large capacitance output and a longer pulse time. Under the condition of the same output amplitude preference, pulse width smaller output curve, so we decided to set up the experiment of the energy storage capacitor part based on the capacitor in parallel.

IV. TRIGGERED ARCHITECTURE ADJUSTMENT

A. TRIGGER CIRCUIT EXPERIMENT

The voltage amplitude generated by the traditional Marx trigger circuit is the voltage that causes the avalanche transistor to enter the avalanche state, which has a smaller amplitude and a wider pulse width. Observed in Fig. (4), in connection with the fitted Equation (1) in the previous experiment and the output at the load end part Equation (3). This may be explained as the increase of stage numbers will lead to the rise of internal resistance, and there is a limit to increasing output amplitude by increasing circuit stages. To improve the circuit's output amplitude, there is a way to enhance the amplitude of the trigger signal. As can be seen from Fig.3, in the discharge phase, the theoretical voltage on the load will be the cumulative voltages of all the energy storage capacitors plus the voltage of the trigger signal. According to Equation (3), all avalanche triodes' internal resistance at the conduction stage will consume a part of the total output, so the voltage applied to the load will have a fixed ratio. Theoretically, as the voltage generated in the Marx circuit has been fixed, and increasing the amplitude of the trigger voltage will increase the corresponding output, which will improve the trigger circuit performance. A high amplitude pulse source is set in the front as the trigger source to provide the trigger signal for the subsequent 40-level circuit. The trigger signal through experiments is then improved and optimized to improve the system's total output.

B. THE EXPERIMENT

According to the previous corollary, the trigger voltage amplitude has a significant influence on the output. To determine the effects of each parameter of the trigger signal on the output result, we increased the circuit levels of the trigger part step by step according to the idea of the previous selection of stage numbers. To observe how the variation of parameters such as trigger amplitude, pulse width, and rising edge influence the output. next, we plot the relationship between the trigger voltage and the output amplitude.

In the experiment, Fig.9 attracts our attention because at about stage 20 of the trigger voltage curve, the following stage trigger output is smaller than the previous output. The smaller trigger voltage generates more significant output than the larger trigger voltage output is contradicts our reasoning. To find out the cause and solve the problem, we analyze the part that has the problem. We compare trigger voltage output curves of stage 19 and stage 20 side by side for better observation.

In the figure, we can see that the highest output amplitude is at the back end of the waveform, and the peak output voltage of stage 19 is greater than that of stage 20. The pulse width and rising edge of both are almost the same. However, in this waveform, we can observe that the most significant

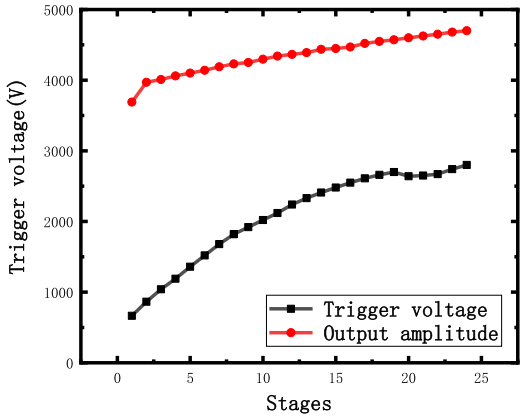

FIGURE 9. Trigger voltage and output amplitude curve.

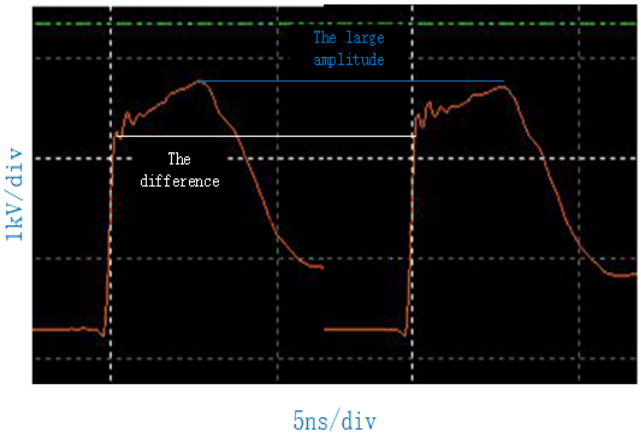

FIGURE 10. Comparison diagram of trigger voltage output curve of stage 19 and stage 20.

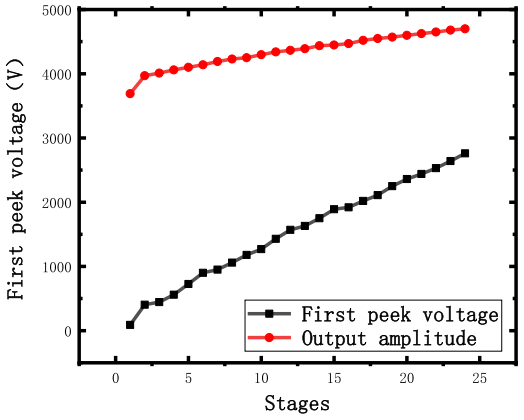

FIGURE 11. First peek voltage and output amplitude curve.

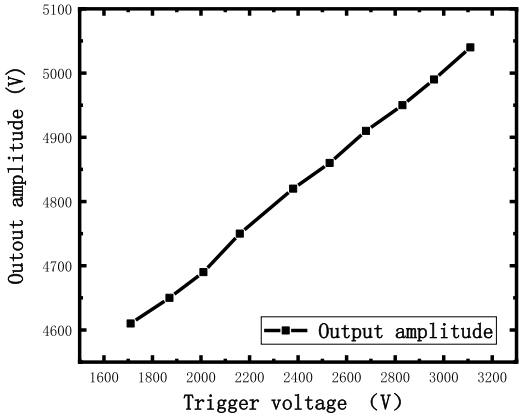

FIGURE 12. After correcting the trigger voltage and output curve.

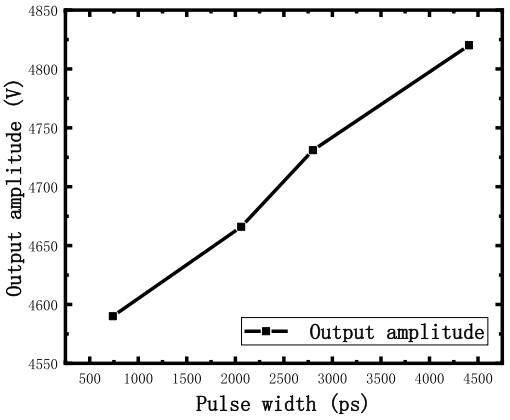

FIGURE 13. Trigger signal pulse width and output amplitude curve.

difference between the two waveforms lies in part marked by the solid white line. The output of the first peak of the two waveforms is different, and the output of the first peak of stage 20 is greater than that of stage 19. Considering our experiment forecast result is about within 1ns pulse width. Fig.10 shows that the rising time is more than 1 ns. According to Marx circuit, instantaneous discharge characteristic, at discharge stage, the rising time is determined by the avalanche transistors' nature, and the rise time is usually very short about hundreds of ps. So we infer that it plays a decisive role in rising fast peak output voltage for the first period, namely, the first rapid increase of peak voltage amplitude which affected the result of the experiment. We then rearrange the output curve for the stages with the first peak output.

To further verify this conjecture's correctness, we set the zero-order Gaussian signal as the trigger signal so that the waveform has only one output peak while ensuring the accuracy of the measurement of the rising time. We set the same pulse width, rising time to change the trigger voltage amplitude experiment.

After the control pulse width and increase the time, the trigger of the output curve, as shown in the figure shows, triggered the first peak of the output signal. This has the most significant influence on the subsequent circuit. Considering if the peak rise time has exceeded the avalanche transistor rise time, at the amplitude of that moment, transistor rise time will affect the output of the circuit. An increase in the output voltage of the peak will lead to trigger the rise in the initial stages resulting in the slope increase, which will improve the output amplitude. During the rise time, the greater the amplitude is, the greater the output will be. Next, we changed the pulse width experiment to control the output amplitude, keeping the time of rising edge to be the same, and the pulse width to observe the output.

As shown in Fig.13, we found that with the increase of trigger pulse width under the same trigger amplitude

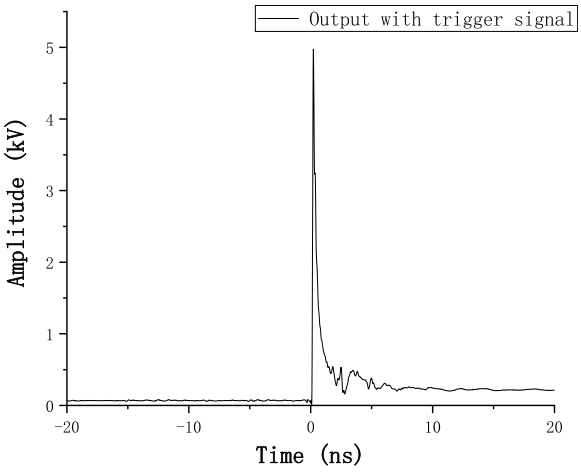

FIGURE 14. Total output of the final circuit.

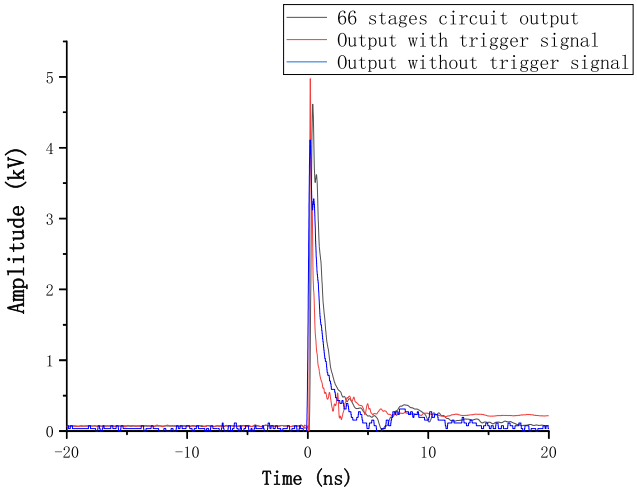

FIGURE 15. Contrast curves of different situations.

condition, the output amplitude increases. Because of trigger pulse width is determined by the capacitance from the trigger circuit, within a specific range of trigger circuit pulse width is smaller, in the control experiments, maintaining the same output amplitude will make the circuit capacitor decrease. At the discharge stage, the capacitors from the Marx circuit and signal source capacitance together form the discharge circuit of the equivalent capacitance will lead to corresponding reductions and the output amplitude will decrease. Refer to Equation (2). So the trigger pulse width has a significant influence on the output pulse width.

To obtain an output signal with a high amplitude and a narrow pulse width, we refer to the Fig.12 and Fig.13 to select a trigger voltage with a wide amplitude and a narrow pulse width. To meet the requirements, we made a circuit with an amplitude of 3160 V and a 4.4 ns pulse width as the trigger signal. The final experimental components were selected as follows: Avalanche transistors were all FMMT415, the current limiting resistance chosen was 10 kΩ, and the capacitances were selected as 6* 47 pF to form the energy storage capacitor group.

Then get an amplitude of 5 kV and a 660 ps pulse width.

When compared with the circuit without the trigger module, it is observed that the circuit without the improved trigger signal increases the series to 66 stages (using the same number of avalanche transistors as the loaded trigger circuit), and the improved trigger signal significantly increases the output amplitude.

It is observed from Fig. 15 that the improved trigger signal has a significant influence on the increase of the output amplitude of the pulse source and could be a possible new direction for further research.

V. THE CONCLUSION

In this work, the application prospects of the current Marx circuit are described considering the limitations in improvements of other circuit forms. We proposed a new Marx circuit trigger configuration that can obtain an output of higher amplitude due to improved traditional capacitance structure. Compared with other parallel circuits with peak output, this circuit ensures a higher peak output voltage while reducing avalanche triodes' usage. Theoretical and experimental study results on a high-voltage nanosecond Marx generator based on avalanche transistors have been presented. The main contributions and findings of this work are as follows:

1. The hierarchical growth curve model of the Marx circuit is tested and drawn step by step, which provides the basis of stage selection for future workers' follow-up research.

2. The circuit configuration of the existing application structures is improved. Through experimental analysis, we proposed the improved design to be a parallel structure of multiple capacitors.

3. A high-amplitude trigger structure was assumed to be helpful to improve the output of the Marx circuit, which was verified by experiments designed to test how the rising time and peak voltage of the trigger circuit influence the output. The optimal parameters were obtained by comparing the results of different experiments. Finally, it is proved that the matching trigger circuit can improve the output of the circuit

The conclusions as well as the complete design process may provide a reference (guideline) to the similar methods of generating high-voltage nanosecond pulses using semiconductor switching devices.

REFERENCES

[1] P. Krishnaswamy, A. Kuthi, P. Vernier, and M. Gundersen, "Compact subnanosecond pulse generator using avalanche transistors for cell electroperturbation studies," *IEEE Trans. Dielectr. Electr. Insul.*, vol. 14, no. 4, pp. 873–877, Aug. 2007.

[2] Q. Wang, X. Tian, Y. Liu, B. Li, and B. Gao, "Design of an ultra-wideband pulse generator based on avalanche transistor," in *Proc. 4th Int. Conf. Wireless Commun., Netw. Mobile Comput.*, Oct. 2008, pp. 1–4.

[3] J. Jethwa, E. E. Marinero, and A. Müller, "Nanosecond risetime avalanche transistor circuit for triggering a nitrogen laser," *Rev. Sci. Instrum.*, vol. 52, no. 7, pp. 989–991, Jul. 1981.

[4] A. Lundy, J. R. Parker, J. S. Lunsford, and A. D. Martin, "Avalanche transistor pulser for fast-gated operation of microchannel plate image-intensifiers," *IEEE Trans. Nucl. Sci.*, vol. NS-25, no. 1, pp. 591–597, Feb. 1978.

[5] A. Omurzakov, A. K. Keskin, and A. S. Turk, "Avalanche transistor short pulse generator trials for GPR," in *Proc. 8th Int. Conf. Ultrawideband Ultrashort Impulse Signals*, Sep. 2016, pp. 201–204.

[6] T. Heeren, T. Ueno, D. Wang, T. Namihira, S. Katsuki, and H. Akiyama, "Novel dual Marx generator for microplasma applications," *IEEE Trans. Plasma Sci.*, vol. 33, no. 4, pp. 1205–1209, Aug. 2005.
[7] M. Rakhee, "Development of cable fed flash X-ray (FXR) system," *Rev. Sci. Instrum.*, vol. 88, no. 8, p. 83307, 2017.
[8] J. Li, Z. Zhao, Y. Sun, Y. Liu, Z. Ren, J. He, H. Cao, and M. Zheng, "A hybrid pulse combining topology utilizing the combination of modularized avalanche transistor Marx circuits, direct pulse adding, and transmission line transformer," *Rev. Sci. Instrum.*, vol. 88, no. 3, Mar. 2017, Art. no. 033507.
[9] X. Yuan, H. Zhang, and B. Yang, "4kV/30kHz short pulse generator based on time-domain power combining," in *Proc. IEEE Int. Conf. Ultra-Wideband*, Sep. 2010, pp. 1–4.
[10] X. Zhang, X. Yang, Z. Li, and H. Yang, "Subnanosecond pulsed power generator with avalanche transistor Marx circuit," in *Proc. Int. Conf. Comput. Problem-Solving*, 2011, pp. 347–349, doi: 10.1109/ICCPS.2011.6089800.
[11] Y. Xuelin, D. Zhenjie, Y. Jianguo, H. Qingsong, Z. Bo, and H. Long, "Research on high-stability pulser based on avalanche transistor Marx circuit," *High Power Laser Part. Beams*, vol. 22, no. 4, pp. 757–760, 2010.
[12] T. H. O'Dell, "Series operation of avalanche transistors," *Electron. Lett.*, vol. 5, no. 5, pp. 94–95, Mar. 1969.
[13] H. Guan, "A Marx high-voltage pulse source based on the series-parallel connections of avalanche transistors," in *Proc. ICCD*, 2017, pp. 1–8.
[14] B. M. Kovalchuk, "Multi gap switch for Marx generators," in *Proc. 13th IEEE Int. Pulsed Power Conf.*, Jun. 2001, pp. 1739–1742.
[15] A. Chatterjee, K. Mallik, and S. M. Oak, "The principle of operation of the avalanche transistor-based Marx bank circuit: A new perspective," *Rev. Sci. Instrum.*, vol. 69, no. 5, pp. 2166–2170, May 1998.
[16] J. C. Pouncey, J. M. Lehr, and D. V. Giri, "Erection of compact Marx generators," *IEEE Trans. Plasma Sci.*, vol. 47, no. 6, pp. 2902–2909, Jun. 2019.
[17] W. Ding, Y. Wang, C. Fan, Y. Gou, Z. Xu, and L. Yang, "A subnanosecond jitter trigger generator utilizing trigatron switch and avalanche transistor circuit," *IEEE Trans. Plasma Sci.*, vol. 43, no. 4, pp. 1054–1062, Apr. 2015.
[18] M. Gao, Y. Z. Xiem, and Y. H. Hu, "Parameter optimization for rise time of sub-nanosecond pulser based on avalanche transistors," in *Proc. IEEE 21ST Workshop Signal Power Integrity (SPI)*, Oct. 2017, pp. 1–3.
[19] J. Li, X. Zhong, J. Li, Z. Liang, W. Chen, Z. Li, and T. Li, "Theoretical analysis and experimental study on an avalanche transistor-based Marx generator," *IEEE Trans. Plasma Sci.*, vol. 43, no. 10, pp. 3399–3405, Oct. 2015.
[20] V. Rai, M. Shukla, and R. Khardekar, "A transistorized Marx bank circuit providing sub-nanosecond high-voltage pulses," *Meas. Sci. Technol.*, 1999, vol. 5, no. 4, p. 447.
[21] Z. Ai, "Nanosecond pulser based on serial connection of avalanche transistors," *Automat. Instrum.*, vol. 2012, no. 5, pp. 61–64, 2012.
[22] M. Gao, Y. Xie, Y. Qiu, Y. Hu, and K. Li, "Performance improvement for sub-nanosecond Marx generator based on avalanche transistors by considering the traveling wave process," in *Proc. IEEE Asia–Pacific Symp. Electromagn. Compat. (EMC/APEMC)*, May 2018, pp. 925–927, doi: 10.1109/ISEMC.2018.8393917.
[23] W. Zhangjing, "Research on key technology of impulse radar," Univ. Electron. Sci. Technol. China, Chengdu, China, Tech. Rep., 2019.

RENJIE HE was born in Nanchong, Sichuan, China, in 1996. He received the B.S. degree in electrical engineering from Guangxi University, Nanning, China, in 2018. He is currently pursuing the M.S. degree with the School of Physics, University of Electronic Science and Technology of China.

His research interests include pulsed-power technology and high voltage pulse technology.

YANG LI was born in Zhengzhou, Henan, China. He received the M.S. and Ph.D. degrees in radio physics from the University of Electronic Science and Technology of China, Chengdu, China, in 2009 and 2014, respectively. He is currently an Instructor with the School of Physics, University of Electronic Science and Technology of China. His current research interests include ultra-wideband antenna and systems, pulsed power systems, and ground-penetrating radar.

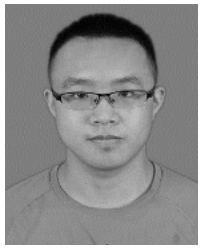

ZHENNAN LIU was born in Ziyang, Sichuan, China, in 1997. He received the B.S. degree in electrical engineering from the Wuhan University of Science and Technology, Wuhan, China, in 2019. He is currently pursuing the M.S. degree with the School of Physics, University of Electronic Science and Technology of China.

His research interests include pulsed power technology and high voltage pulse technology.

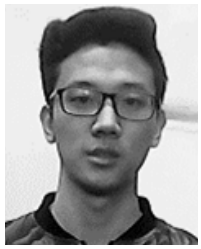

JIAHAO JIN was born in Yuncheng, Shanxi, China, in 1998. He received the B.S. degree in electronic information from the University of Electronic Science and Technology of China, Chengdu, China, in 2019, where he is currently pursuing the M.S. degree with the School of Physics. His research interest includes pulsed power technology and its applications.

ZHENGCHUN SUN was born in Xi'an, Shaanxi, China, in 1996. He received the degree in electronic information engineering from the Xi'an University of Posts and Telecommunications, Xi'an, in 2018. He is currently pursuing the master's degree in electronic and communication engineering from the University of Electronic Science and Technology of China, Chengdu, Sichuan, China. His research interest includes pulsed power technology and its application.